AN ABSTRACT OF THE THESIS OF

Chad L. Butler for the degree of Master of Science in Mechanical Engineering presented on June 4, 1996. Title: The Application of Ablative Laser Ultrasonics to an Aluminum Plate, Titanium Tube, and Welded Joints

Abstract approved: Redacted for Privacy

Clarence A. Calder

Laser ultrasonics can be used to nondestructively evaluate structures to determine the existence and location of surface and interior flaws. The goal of this research was to determine if laser ultrasonic techniques can be applied to the inspection of aluminum plate, titanium tubes, and large welded plate structures. The research was carried out with a Q-switched pulsed ruby laser emitting light of 694 nm wavelength. Ultrasonic waves were experimentally generated and recorded in the aluminum plate and the titanium tube. A comprehensive literature study was completed to determine if the technique can be applied to welded structures. For the two experimental cases, the ultrasonic waves were received by a piezoelectric pinducer which was located on the opposite side of the plate, and on the outside of the tube. A digital oscilloscope captured the signals from the pinducer. The signals were then analyzed to determine echo spacing and frequency content. The physical characteristics of the laser pulse such as the energy and full-width-half-height and amplitudes were measured via a photodiode system and a calorimeter. The aluminum plate confirmed that the system was functioning properly, as the ultrasonic echoes that were generated matched the expected results from previous experimentation. The titanium tube data turned out to be difficult to interpret due to the complex geometry and mode conversion. The welding research showed that ultrasound can be used to identify many types of flaws in a welded joint. Currently, few researchers have applied the laser based ultrasound to flaw detection in finished welds, although several have looked at using the laser ultrasound as an input to a control system for a weld in progress. The literature research uncovered the need for further studies on the application of laser based ultrasound to flaw detection in completed welds.

The Application of Ablative Laser Ultrasonics to an Aluminum Plate, Titanium Tube, and Welded Joints

by

Chad L. Butler

A THESIS

submitted to

Oregon State University

in partial fulfillment of

the requirements for the

degree of

Master of Science

Completed June 4, 1996

Commencement June 1997

Master of Science thesis of Chad L. Butler presented on June 4, 1996

APPROVED:

Redacted for Privacy

Major Professor, representing Mechanical Engineering

Redacted for Privacy

Chair of Department of Mechanical Engineering

Redacted for Privacy

Dean of the Graduate School

I understand that my thesis will become part of the permanent collection of Oregon State University libraries. My signature below authorizes release of my thesis to any reader upon request.

Redacted for Privacy

Chad L. Butler, Author

Acknowledgment

I would like to thank Gunderson Metals of Portland for their financial contributions to this research. I am grateful to Dr. Calder for providing the equipment and experience necessary to complete the project. I am in debt to Dr. Reistad and other members of the department who supported me through this endeavor. To my family who has always been there for me, thanks for your support as well.

TABLE OF CONTENTS

TABLE OF CONTENTS (Continued)

Page

LIST OF FIGURES

LIST OF FIGURES (Continued)

Figure Page

The Application of Ablative Laser Ultrasonics to an Aluminum Plate, Titanium Tube, and Welded Joints

Chapter 1

Introduction

1.1 Background:

When Einstein first suggested the idea for stimulated emission of light in 1917, no one at that time could have predicted the practical applications and the changes that would come. Founded on Einstein's principles, the maser (microwave amplification by the stimulated emission of radiation) was created in the early 1950's. The maser was developed by Charles H. Townes. The race was on to apply the same idea to electromagnetic radiation in the visible light wavelengths. It was not until 1960 that Theodore Maiman discovered the laser (light amplification by the stimulated emission of light).[1] He was working at Hughes research labs in Malibu, CA. Maiman developed the pulsed ruby laser which emits light at a wavelength of 694 nm. Three years later in 1963, White first suggested the idea of the generation of acoustic pulses with a laser focused on a metal surface. White not only tested lasers, but electron and microwave radiation to see if any type of electromagnetic radiation would generate elastic waves.[19] White's ideas set the groundwork for the field of laser ultrasonics which exists today. The fundamental principles of hitting a surface with a laser and generating elastic waves has not changed, but the means of detection and the variety of lasers and power ranges available today has allowed for a broad spectrum of applications.

Laser ultrasonics can be used in either a thermoelastic regime, or an ablation regime. In each of these regimes, a different mechanism generates the elastic waves that propagate through the medium. The local power density applied to the surface by the

laser impulse controls whether ablation or thermoelastic effects dominate. The threshold power density in order for ablation to occur is a function of the material's melting temperature, the temperature at the surface before lasing, the density, time duration of the shot, thermal conductivity, surface reflectivity, and the specific heat of the material. For aluminum, this threshold value turns out to be on the order of 10^7 W/m^2. If the power density is below this threshold, then thermoelastic effects dominate. In the thermoelastic regime the energy imparted to the surface is enough to cause local heating and expansion. This expansion works against the inertia of the sample and produces stresses at the boundaries of the heated region. This results in the propagation of elastic waves in the material. In the ablative regime, the energy imparted to the surface causes subsequent liquefaction, heating and vaporization of the surface layer. A hot plasma is ejected from the surface. The reaction between the hot expanding plasma and the surface produces a stress pulse to be generated due to the momentum exchange.

Ablation generates three types of elastic waves simultaneously. They are dilatational, shear, and Rayleigh waves. They differ in their mode and velocity of propagation through the medium. Dilatational waves have particle displacements in the same direction as the axis of propagation of the wave. An example of a dilatational wave is a sound wave which consists of zones of compression and rarefaction, as is shown in figure 1. The wavelength is defined as the distance between points where the particles are in the same state of motion.[5] For example, the distance between two compression zones can be taken as the wavelength. Compression zones are zones of dense lines in Figure 1. Shear waves have particle displacements perpendicular to the direction of propagation of the wave. Shear waves only propagate efficiently through solid bodies because fluids are unable to sustain shear without deformation. An example of a shear wave is shown in figure 1.

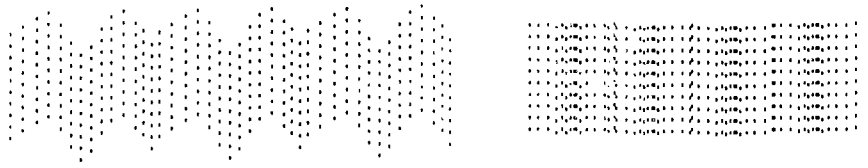

a) Shear Wave b) Dilatation or Longitudinal Wave

Figure 1. Shear and Dilatational Wave Diagrams [5]

The particles in the shear wave oscillate along the vertical axis however the wave is propagating along the horizontal axis. The velocities of propagation of the dilatational and shear waves in a medium is dependent on the elastic properties of the medium. The shear waves travel at a velocity of approximately half that of the dilatational waves. In Al the ratio of C_T/C_L is 0.49, where C_T is the shear wave velocity and C_L is the longitudinal wave velocity. The velocities of the ultrasonic waves in a material are temperature dependent. The third type of wave that is generated by ablation is the Rayleigh waves or surface wave. They propagate only along the surface of a material and spread out only in two dimensions. In Rayleigh waves, the particle motion has components in both the direction of wave propagation, and the direction perpendicular to the direction of wave propagation. A common example of a Rayleigh wave is found in earthquakes. Rayleigh waves propagate slower than the dilatational waves and the shear waves as they spread out from the epicenter. They have the greatest amplitudes because geometric spreading and attenuation occur in two dimensions instead of three.

In this research the ablative ultrasonic regime was used in the evaluation of Ti tube and an Al plate for nondestructive evaluation of the materials. A pulsed ruby laser was used to generate the elastic waves, and piezoelectric transducers were used to receive the ultrasonic signals. Pitch-catch methods were employed in which the source of ultrasonic wave generation and the receiving piezoelectric transducer were physically separated. The laser pulse characteristics were analyzed. This included the full-width-half-height of the pulse, as well as the energy value per pulse. The energy value per pulse of the laser was measured with a calorimeter designed for absorbing laser energy of the ruby wavelength. Once the pulse characteristics were determined, then the triggering system was modified

from the previous setup. A fast photodiode was set up to trigger data acquisition by the oscilloscope. This allowed for precise timing of the laser firing and the pulse arrival at the far end of the sample. Then the ultrasonic testing was performed on an Al plate to ensure that the apparatus was working properly. The Ti tube was used to see what type of ultrasonic output resulted when lasers were used to instigate the ultrasonic wave propagation in the medium.

1.2 Literature Review:

1.2.1 *Applications*:

The field of laser ultrasonics is making flaw detection and nondestructive evaluation possible in areas that were previously too difficult to monitor. Testing of parts at elevated temperatures with conventional ultrasonics is difficult because a couplant layer must be maintained between the part and the measurement transducer. Moving parts that are being transported on assembly lines are also difficult to inspect because of the translational movement of the belt. The transducers themselves are phase sensitive devices which emit from their whole surface. This means that they must be aligned very carefully in order to minimize errors.[3] Also inspection of curved surfaces with conventional ultrasonics requires contour following devices which make practical inspection difficult. Laser ultrasonics produces ultrasonic waves which propagate perpendicular to the surface, even if the laser beam is oriented at an angle with respect to the surface. This makes inspection easier because the laser beam does not have to be oriented perpendicular to the surface.

Laser based ultrasound inspection (LBU) on a surface requires the use of two lasers. One induces the ultrasonic waves in the material, and another laser is used as an interferometer to measure the movement of the surface caused by the ultrasonic waves in the material. Laser ultrasonics is being studied to find cost effective uses in industrial

applications. Combinations of lasers and piezoelectric transducers can also be used in industry. One example of this is in the analysis of large metal ingots common to the metals industry to detect internal flaws. A large metal Ti remelt section was tested with ablative ultrasonics with a Q-pulsed ruby laser. Pinducers were used to measure the resulting ultrasonic waves in the material. The small 2.5mm diameter of the pinducer used makes field use on rough surfaces possible. [21] The technique was used to evaluate flaws in the material. The use of LBU has become popular, and in certain cases due to operational environment it is the preferred method since it does not require contact with the specimen under study. An example of this is in the thickness gauging of hot tubes as they are being manufactured. Monchalin studied A36 steel tubes which were at 1000^0C. Assuming a velocity of propagation in the steel for dilatational waves of 4900m/s the thickness of the steel was calculated.[3] This allows for tuning of the manufacturing process to attain desired tolerance on the thicknesses coming off the line. The tubes were then cooled and measured with conventional ultrasonic techniques and the two methods were compared to validate the results of the ultrasonic measurements. Another application that is suited ideally for laser ultrasonics is the rapid inspection of composite plates. A laser ultrasonic system has been designed to scan composite surfaces for damage from a distance of five feet away.[3] A curved graphite epoxy composite covered by a metallic mesh for protection against lightning was scanned with a laser ultrasonic system. This produced a two dimensional image of the composite plate with the imbedded flaws becoming apparent in the scanned images. This is the type of research that demonstrates the power and advantages of the laser ultrasonic system.

Other applications include the search for methods of flaw detection in thin sheets of metal. One of the difficulties in using laser based ultrasonics on very thin materials is that waves of several different modes propagate down the medium. In order to only excite and propagate one mode, a method has been used in which two laser beams of different frequencies are focused at the same spot. The Rayleigh waves that result are of a precise frequency determined by the difference in frequency of the two generation lasers.[27] This type of method allows for line scanning of a sheet where the generation and receiving lasers are on opposite sides of the metal sheet and are scanned parallel to each other once

across the sheet. This method takes considerably less time than doing an XY surface scan on the same sheet.

A microchip laser has been investigated to be used as a receiver for ultrasonic signals that are generated in a medium. This is a novel technique in which one end of the microchip laser is attached or coupled to the surface, and the ultrasonic waves cause a frequency modulation of the laser beam that exits the cavity. The ultrasonic waves modulate the beam by physically changing the cavity length with respect to time. This beam can then be demodulated to obtain the displacement information of the acoustic field that impinged on the laser. [26] This is expected to have applications in the medical field.

1.2.2 *Detecting Defects in Carbon Fiber Matrix Composites*:

Laser ultrasonics is currently being used to investigate defects in large composite sheets. The sheets appear on commercial and military aircraft. Often the defects are inside and there is no visible damage on the outside of the surface. For composites, the ultrasonic generation efficiency is a function of the optical absorptivity of the resin, and the reinforcing fibers, plus the absorptivity of any coating placed on the surface.[7] The optical absorption of the resin can be a function of the wavelength of the laser energy imparted to the surface. All materials absorb electromagnetic radiation. The light photon hits the surface and the electric field interacts with the surface atoms raising them to an excited energy state. This process occurs at the resonant wavelengths, and the energy is dissipated as heat in the solid. [11]

One of the difficulties in LBU is determining how much light is scattered versus the amplitude of signal that has been lost due to attenuation in the medium. What is done to counteract this is to phase modulate one of the mirrors in the interferometer with a piezoelectric transducer. This produces a signal that has a constant frequency. However, the amplitude of the signal is completely dependent on the amount of light collected.

During manufacturing, 10 mm range defects were placed in a flat carbon fiber sheet, and the sheet was scanned with the LBU system. A Nd:YAG laser was used to

generate the ultrasonic waves. All of the planted defects were found by the system including an unexpected 12x2 mm defect that was created during the manufacturing process. The data was verified using conventional ultrasonic scanning systems. The same type of scan test was performed on a carbon fiber hat section to locate the flaws in that type of geometry. The scan located all eight of the implanted flaws. This geometry is shown in Figure 2. [7]

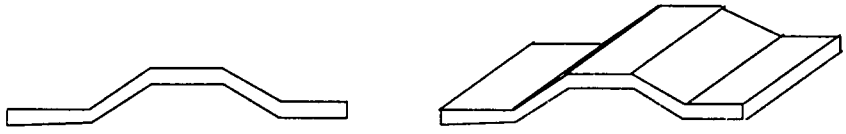

Figure 2. Top Hat Section Geometry [7]

In addition to dilatational scan methods, another researcher is investigating the use of Lamb waves to detect defects in carbon fiber plates in the 10-20mm size category. Since Lamb waves travel over large distances, a line can be inspected at each transducer position instead of a single point. Carbon fiber-reinforced plastic specimens were used and they were 600mm long by 90mm wide, with a thickness of 1mm. [8] A delaminated area was created in the specimens at a length of 400mm from the transducer and the reflection of the Lamb wave from the defect was detected. In order for this method to be used in industry, further research would have to be done and transducer technology improved so reflections inside the transducer are not mistaken for defects. Lamb waves are also measured by an Optical Beam Deflection technique in which the waves are detected using light gathering optics catching the reflected light from a source laser. [13] Researchers are using techniques such as this one to avoid contact with the surface and develop purely non-destructive testing methods.

1.2.3 *Material Property Evaluations*:

In order to determine the torsional vibration frequencies of a long slender rod. The rod was impacted with a metal ball at the end which produced a broad bandwidth of vibrational frequencies in the bar. The vibration was detected at a point with an interferometer. The frequency content of the signal was evaluated for the eigenfrequencies. Thus interferometry led to the determination of natural frequencies for the bar. [12] Interferometry is an integral part of the laser based ultrasound systems. Another use of laser ultrasonics methods is in the determination of elastic constants and their dependence on temperature. A single crystal semi-conductor and a poly-crystalline metal were investigated for the dependence of the surface wave velocities as a function of temperature. This method can be used to determine the elastic constants of the material to within 0.1% certainty. [14] By using laser ultrasonics the motions of the surface are not disturbed by the measuring medium. When the sample expands due to heating the distance between the generation and receiving lasers can be maintained constant, as both lasers are illuminating the same surface. The temperature dependence of the longitudinal ultrasonic velocity in iron and Dural has been investigated through experimentation. [16] Sample disks were placed in an evacuated oven with windows on either side to allow for an interferometer laser and a source laser. As the temperature increased up to 1000°C the velocity was found to decrease and hence the elastic constants change due to their relationship to the ultrasonic wave propagation.

Similar work was done much earlier by Calder in the determination of elastic constants through laser ultrasonics.[35] A clamshell oven was used to vary the temperature of rod samples, and the ends were open to the atmosphere providing convenient access for the generation and interferometric lasers. Six metals were studied. They were aluminum, steel, copper, brass, tanalum, and molybdenum. The first longitudinal pulse and successive mode converted pulses were captured with an oscilloscope. From this data the elastic constants of the materials were measured with respect to variations in temperature. Calder showed that a linear relationship between temperature and the elastic properties of the metals existed in all six cases. The elastic

properties decreased with increasing temperature. Calder also found the elastic properties of plutonium and delta-stabilized plutonium over a temperature range from ambient to near the melting point. The same technique was used with the clamshell oven and noncontact laser approach. [36]

Laser ultrasonics is also used to measure the elastic constants of composites formed by powder metallurgy. The materials have porosity, density variations, and secondary phases, all of which make ultrasonic methods preferable. [17] The material was placed between a source laser and an interferometer laser and the shear and dilatational wave velocities were measured. From these velocities the bulk modulus, B, and the shear modulus, G, can be calculated as is shown in the following equations.[18]

$$B = \left(v_l^2 - \frac{4 v_s^2}{3} \right) \qquad (1.2.3.1.)$$

$$G = \rho v_s^2$$

where ρ is the density

v_s is the shear wave velocity

v_l is the longitudinal wave velocity

Due to the hardness of some tungsten carbide, cobalt metals formed from sintered powders, conventional methods of determining the elastic constants were possible only with diamond tools. [17] Since this is expensive and produced inconsistent values, the laser ultrasonic techniques were successfully applied.

1.2.4 *Noncontact Detection of Laser Ultrasonic Signals*:

Current research is directed to develop an accurate and cost effective noncontact measuring system to record the ultrasonic pulses that the laser generates in the material. Monchalin has been using the Confocal Fabry Perot Interferometer. [3] One difficulty in designing a system to record the ultrasonic wave pulses using optical techniques is that the

intensity of the reflected light varies. Discriminating between ultrasonic fluctuations and light intensity fluctuations is no trivial matter. Monchalin managed to do this with his confocal fabry perot system and electronics.

Other techniques have been used to solve the same problem. For example, fiber optic cables have been used to transmit and receive the interferometric laser light from the surface. The bundle of fibers that collects the light was split into two groups of fibers, and the output from each bundle was taken to a separate photodiode. Then the output from the two photodiodes was compared with a differential amplifier circuit. [25] This method gave consistent results even when the intensity of the light varied as expected in the scanning of a surface. Another sensing method of tackling the same problem was based on the theory of injection locking. A small amplitude of light at a certain frequency is accepted into a laser cavity, and the cavity amplifies the intensity, while maintaining the phase information that was contained in the incoming light. This produces a constant output, yet the intensity of the incoming light can vary. In order to extract the information, that laser beam is mixed with another and the resulting light is demodulated to obtain the displacement information of the surface.[24] The current trend seems to be a race to find a method of noncontact detection of the displacement of the surface which is economical and does not have to be aligned very carefully, and can withstand fluctuations in the light intensity of the reflected light from the surface.

Chapter 2

Theoretical Background

2.1. Wave Velocity:

In a bounded isotropic elastic solid three types of waves can propagate. They are dilatational, shear, and Rayleigh waves. The waves propagate at specific velocities depending on elastic properties of the material. Anything that effects the elastic properties of the material influences the velocity of elastic waves in the material. For example, increasing the temperature generally decreases the stiffness of the material which causes a decrease in the velocity of wave propagation in that material. The wave velocities are independent of the frequency of the wave. However, the attenuation of a wave is highly frequency dependent, so a wave of a certain frequency may propagate through a solid, but not be measurable because of attenuation.

A linear elastic solid is defined by five parameters. In order to be a linear elastic solid, the relation between the applied loading and the deformation must be linear. The rate at which the load is applied does not have any effect. By removing the load the solid must return to its original state as the deformations go to zero. The applied deformations are very small, and the material must be homegenous in nature. The homogenous material implies that the constants in the stress strain equations are independent of position.

The stress in a sample is defined as the force per unit area. For example, if a stress is denoted by σ_{ij} , the first subscript (i) in the notation of stress denotes the direction in which the stress acts, and the second (j) denotes the plane in which it acts. The strain is defined as a change in length with respect to the original length. The strain relations show how a point whose original position was defined as (x,y,z), and after an applied loading situation the coordinates become (x+u, y+v, z+w). The relative change in position between the two points is the strain in the sample and is denoted with the following notation.

$$\varepsilon_{xx} = \frac{\partial u}{\partial x} \quad \varepsilon_{yy} = \frac{\partial v}{\partial y} \quad \varepsilon_{zz} = \frac{\partial w}{\partial z}$$
$$\varepsilon_{xy} = \frac{1}{2}\left(\frac{\partial v}{\partial x} + \frac{\partial u}{\partial y}\right) \quad \varepsilon_{xz} = \frac{1}{2}\left(\frac{\partial w}{\partial x} + \frac{\partial u}{\partial z}\right) \quad \varepsilon_{zy} = \frac{1}{2}\left(\frac{\partial w}{\partial y} + \frac{\partial v}{\partial z}\right) \tag{2.1.1}$$

Once the quantities of stress and strain have been defined, it is then possible to show how Hooke's law relates the two quantities. The relationship between stress and strain is known as Hooke's law for linear elasticity. In its most general form it contains 81 independent constants and nine equations which can be expressed in the form of equation 2.1.2.

$$T_{ij} = C_{ijkl} E_{kl} \tag{2.1.2}$$

where T is the stress tensor

E is the infinitesimal strain tensor

and i,j = 1,2,3

Because the strain tensor is symmetric $E_{ij} = E_{ji}$ the number of independent constants reduces to 54. The stress tensor is also symmetric $T_{ij} = T_{ji}$ which reduces the number of constants from 54 to 36 constants. This leaves 36 constants in the equations, and only 18 of those are independent. [22]

According to Hooke's law each of the six independent components of stress is a linear function of six components of strain. If a point in a solid body is chosen, there are actually nine components of stress acting on that point. However, only six of these stress components are independent because $\sigma_{xy} = \sigma_{yx}$ $\sigma_{yz} = \sigma_{zy}$ $\sigma_{zx} = \sigma_{xz}$. Thus this leads to the set of 36 constants above. When a strain energy density function U can be defined, the number of constant coefficients can be further reduced down to 21.

$$T_{ij} = \frac{\partial U}{\partial E_{ij}} \tag{2.1.3}$$

If a solid is then modeled as isotropic, the number of constants further reduces down to only two independent constants. An isotropic solid means the material properties are the same in all directions. The values of the constant coefficients are independent of the axis system. The resulting two independent constants which describe the medium are known as Lame's constants λ and μ. The equations for the elastic medium then reduce to a simpler set of equations as given in 2.1.4.

$$\sigma_{ij} = \lambda \Delta \partial_{ij} + 2 \mu \varepsilon_{ij}$$
$$\Delta = \varepsilon_{ii} \qquad (2.1.4)$$

. In equation 2.1.4., the symbol Δ is know as the dilatation and it physically represents an infinitesimal volume change of the material. These equations will be used in conjuction with the equations of motion in an elastic medium to determine the propagation velocities of waves in a given material. The equations of motion for a material are valid under any stress-strain behavior of the medium. They are derived with a force balance on an infinitesimal cube using Newton's second law F=MA. The resulting equations are as follows.

$$\rho \ddot{u}_i = \sigma_{ij,j} \qquad (2.1.5)$$

In order to solve these equations, one must substitute the elastic relations that were derived earlier. In place of the stress symbols in the above equations the stresses in terms of the elastic constants and strains are substituted. The definitions of the strains are then substituted in the appropriate place. The equations are then mathematically manipulated and placed in the form of equations 2.1.6.

$$\rho \frac{\partial^2 \Delta}{\partial t^2} = (\lambda + 2\mu) \nabla^2 \Delta$$
$$\rho \frac{\partial^2 u}{\partial t^2} = \mu \nabla^2 u \qquad (2.1.6)$$

These equations can be solved directly for the propagational velocities of sound waves in an isotropic, linearly elastic medium. The resulting equations 2.1.7. are the solution of 2.1.6. for the longitudinal and transverse wave velocities.

$$c_L = \left[\frac{(\lambda + 2\mu)}{\rho}\right]^{1/2}$$
$$c_T = \left[\frac{\mu}{\rho}\right]^{1/2} \qquad (2.1.7)$$

where C_L is the longitudinal velocity

C_T is the transverse wave velocity

λ is Lame's constant

μ is shear modulus

ρ is the material density

These are the propagational velocities of the dilatational and shear waves in the medium. Note the shear modulus and the lamda are the only two constants in the equations. The equations can be written in terms of Young's modulus, the bulk modulus, and poisson's ratio, since all the elastic constants are interrelated. A dilatational or shear wave traveling in an isotropic elastic medium must propagate with one of the two velocities. This is a fundamental concept, because the velocity of propagation of the waves can be measured experimentally, and this can be used to determine the elastic properties of the material. In cases where the material is at elevated temperatures, or is difficult to machine and test in the usual manner, this technique is of great importance. Hence, if one knows the elastic properties of a material and the velocity of wave propagation, and an echo comes back before the reflection from the back surface of an object, then this echo can be related to a flaw. This allows for the whole concept of

nondestructive evaluation of a material by laser ultrasound. It is of foremost importance to realize the interactions between wave mechanics and material properties.

2.2 Ablation:

Laser generation of the elastic waves has been classified into two regimes depending on the amount of lasing energy applied to the surface. They are the thermoelastic regime and the ablation regime. For the purpose of this research the ablation regime of laser ultrasonics was used. In the ablative regime, the rate at which heat is supplied to the surface is too fast for appreciable heat conduction away from the surface. This causes an amount of metal and oxide to be vaporized on the surface. This mass is ejected away from the surface and becomes a plasma. Due to the conservation of momentum this action can be modeled as placing a uniform stress on the surface in a very short amount of time. This generates elastic waves in the material.

The thermoelastic regime creates ultrasonic waves in the medium through a different mechanism. The thermoelastic regime uses lower energy densities than the ablation regime, and longer light pulses on the surface. This allows a volumetric expansion of the area under laser illumination. This expansion creates ultrasonic waves in the material without burning off a thin layer of the metal as in the ablative regime. This area is of particular interest when it comes to composite structures and much research is being done to apply thermoelastic laser ultrasonics to composite structures. When using a polymer matrix material, the laser light actually penetrates below the surface depending on the adsorption coefficient of the material involved. This creates a buried source of ultrasonic waves when it comes to modeling this interaction.

In order to produce ablation, a threshold energy density must be deposited on the surface. For most metals the threshold energy density is 10^7 Wcm^{-2}. This threshold energy density, I_c, can be determined by equation 2.2.1.

$$I_c \geq 2L\rho K^{0.5}\tau^{-0.5} \qquad (2.2.1)$$

where L is the latent heat to vaporize the solid

ρ is the mass density of the material

K is the thermal diffusivity

For energy levels above that threshold energy a certain amount of material is removed. The rate of material removal equation is given by equation 2.2.2.

$$\xi = \frac{I}{\rho[L + c(T_v - T_o)]} \qquad (2.2.2)$$

where I is the incident power density

c is the specific thermal capacity of the material

L is the latent heat of vaporization of the solid

T_v and T_0 are the vaporization and initial temperature of the solid

The term zeta describes the rate at which mass is removed from the sample. The mass removal produces a change in momentum which leads to a net stress being applied to the surface. The net stress on the surface can be calculated with the following equation.

$$\sigma = \frac{I^2}{\rho[L + c(T_v - T_o)]} \qquad (2.2.3)$$

where σ is the net stress on the surface

The stress is dependent on the density of the material, the intensity of the energy deposited on the surface, the specific thermal capacity of the material, the latent heat of vaporization, and the temperature initially and at vaporization. These are all known properties of a given material. The only changing factor is the energy power density deposited on the

surface. When an impulsive stress is applied to the surface, ultrasonic waves are generated.

Plasma is formed over the surface, after only part of the incident light pulse has hit the surface. Once the plasma forms, it does several things. It absorbs light from the laser pulse acting as a shield to the incoming light and in doing so it becomes very hot. The plasma also exerts a high pressure on the surface which suppresses the vaporization of the material by raising the boiling point. The plasma also produces an impulse reaction on the surface. The hot plasma radiates some heat back to the surface which maintains a high surface temperature for some time after the initial laser pulse. When the plasma first forms and expands it creates a shock compression front followed by a rarefaction. This phenomenon was observed and studied with a PBD (probe beam deflection) setup by Hrovatin.[6] Above 10^8 Wcm^{-2} the amplitude of the shock wave begins decreasing. There is a critical energy above which the formation of ultrasonic waves becomes less efficient.

2.3 Attenuation:

Now that the wave velocities have been defined it is important to explain the mechanisms that attenuate these waves when they are traveling through the medium. Attenuation is a mixture between scattering and absorption. The scattering is caused by inclusions, cracks or grain boundaries that the stress waves come in contact with. In the case of grain sizes less than 1/100th of the wavelength, scattering due to grain boundary effects can be considered negligible.(5) Inclusions and cracks in the material have boundaries over which the acoustic properties are different and the waves are scattered from the interface. Another means by which attenuation occurs is adsorption. Adsorption is the conversion of mechanical energy of the wave into heat. This can happen by a number of different mechanisms, one of them being hysteresis losses. Real solids are never perfectly elastic. Another mechanism is the temperature gradients that are set up by the compression and dilatational cycles that move through the medium. Velocity gradients

result in losses of energy as well. Geometric spreading attenuates the waves by an inverse square law in three dimensions. Energy is also adsorbed by the medium. Another factor in wave attenuation is the frequency. Higher frequency waves are attenuated much faster in metals than lower frequencies. Frequencies above 10MHz can only penetrate a few centimeters in some metals. The waves are constantly being attenuated by various mechanisms as they move through the medium. This presents a difficult problem to the researcher. By increasing the amplitude of the initial acoustic signal to overcome attenuation, one also increases the level of noise proportionally. The only way to get around this is to lower the frequency of the ultrasonic waves. By lowering the frequency, one has to make tradeoffs on the size of the flaw that can be detected. Scattering is modeled with an exponential law given by equation 2.3.1.

$$I = I_o e^{-\alpha d} \qquad (2.3.1)$$

where α is the attenuation coefficient

d is the depth of the test section

The mechanics of attenuation are such that transverse and longitudinal waves will be effected differently. Cast steel produces stronger attenuation than cold worked or rolled steel even with the same grain size. Attenuation usually increases with temperature.

2.4 Mode Conversion:

When a plane wave strikes a boundary between two mediums, it produces a reflected wave and a transmitted wave. For the case of a solid or liquid with air this is referred to as a free boundary. If a longitudinal wave, L, is incident on the boundary, both a longitudinal and transverse wave are reflected from the boundary. This concept can be seen in figure 3. The converse is also true. When a transverse wave, T, is incident on the boundary of steel and air from the steel side, the wave is reflected and part of the energy is converted into a longitudinal wave.

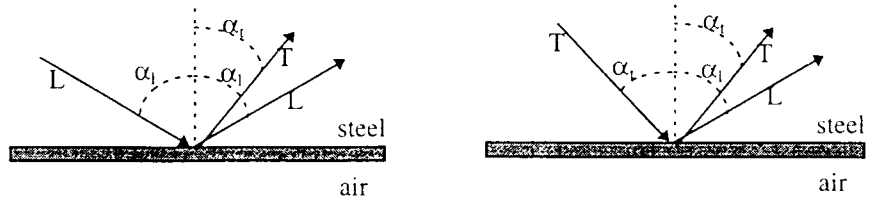

Fig 3. Mode Conversion at Steel Air Interface

The angles of reflection can be calculated using Snell's law of refraction and setting the right hand side equal to the ratio of the stress wave velocities between the transverse and the longitudinal waves.

$$\frac{\sin(\alpha_T)}{\sin(\alpha_L)} = \frac{C_T}{C_L} = 0.55 \qquad (2.4.1)$$

Thus, if the incident angle of the transverse or longitudinal wave is known, the angle of the reflected mode-converted wave can be calculated. For the incident transverse wave where α_t is greater than 33 degrees, the sine term comes out to a value greater than one. This means that the transverse wave was totally internally reflected.

2.5 LASER Principles:

In order to understand how a laser works one must first understand the fundamental principles of light itself. Christian Huygens argued that visible light was made up of waves, whereas Isaac Newton argued that light was made up of tiny particles. In essence both theories are correct. Visible light is an electromagnetic wave which is defined by its wavelength and frequency. The two quantities are related by the speed of light , c.

$$c = \lambda * \nu \qquad (2.5.1)$$

where $c = 10^8 m/s$

Frequency is the number of cycles per second or Hertz named after Heinrich Hertz the discoverer of radio waves. Visible light also acts as though it is made of tiny massless particles or photons. A photon is a quantum of energy.

$$\text{Photon Energy} = h\nu \qquad (2.5.2.)$$

where h is Planck's constant

ν is the frequency.

Visible light has wavelengths in the 400-700 nm range. In order to fully understand lasers one must know that atoms can only have discrete amounts of energy which are defined as states or levels. The laser operates by stimulating atoms to go from one energy state to another all at the same time. This produces a release of energy in the form of radiation. Energy absorbed or omitted equals the difference in energy between initial and final states. The simplest model is a three level laser having three states E_0, E_1 ,and E_2. If E_0 is the ground state then the atoms are irradiated with a known frequency to increase their energy levels to a higher state. $h\nu_p = E_2 - E_0$. This phase is known as pumping the medium and putting energy into the system. This can also be done by electric currents as well as light illumination. The atoms are then irradiated with a different frequency of radiation to stimulate the atoms to drop from one level to another. When this happens, in a controlled fashion radiation of the same frequency is released by a process of stimulated emission. $h\nu_S = E_2 - E_1$

The ruby laser is an example of a three level laser. The Zenon flashlamp excites the atoms from their ground state to a highly excited upper level. From the excited upper level the atoms drop to a metastable state and then the stimulated emission occurs between the metastable level and the ground state. Figure 4. shows a diagram of this process for a

three level laser. The laser transition occurs between a metastable level and the ground state. A tremendous amount of energy is required to create a population inversion where a majority of the atoms are not in their ground state. This makes the process inefficient and that is why solid state ruby lasers operate in pulsed mode.

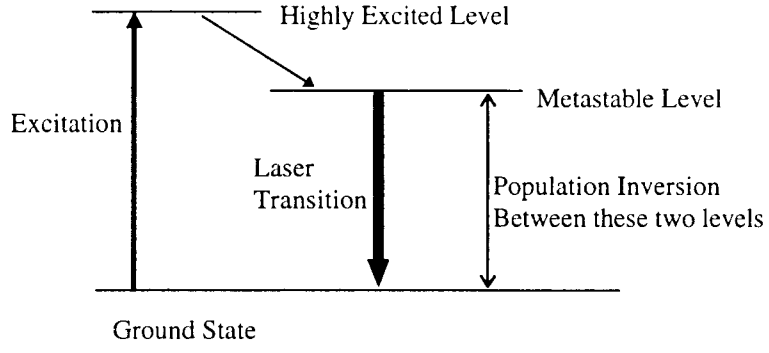

Figure 4. Three Level Laser [1]

Spontaneous emission happens in the sun, stars, fluorescent lamps in which light is emitted at many different frequencies and phases. Stimulated emission results in light of a single frequency and phase. Stimulated emission is the physical process of a photon hitting an excited atom and the atom releases another photon at that same wavelength. In order to produce stimulated emission a population inversion has to be reached. In thermal equilibrium atoms tend to be in their lowest energy states. In order to have stimulated emission this has to be reversed. A higher percentage of the atoms must be in higher energy states in order to produce a cascade of photons. Reversing what is found in nature is known as a population inversion. It can be done with electricity or radiation at a specific frequency. Years ago it was believed that this could not happen. Physicists thought that it was physically impossible to create a population inversion because working backwards through equation 2.5.3. relating populations between energy states gives a negative temperature if E_2 is larger than E_1.

$$\frac{N_2}{N_1} = \exp\left[-(E_2 - E_1)/kT\right] \qquad (2.5.3)$$

where k is Boltzman's constant

T is the temperature.

N_2 and N_1 are the number of atoms in the energy states.

2.6 Piezoelectric Transducers:

A piezoelectric material has the property that if an external deformation is applied to its surface, electrical charges are produced on the surface.[5] The converse is also true that if a charge is applied to the surface, mechanical deformations result. This is known as the piezoelectric effect. If the surfaces are coated with metal, the charge q that develops results in an output voltage according to equation 2.6.1..

$$q = v_o * C \qquad (2.6.1)$$

where v_o is the output voltage

C is the capacitance of the piezoelectric material

The charge q can be related to the applied pressure by the relation.

$$q = SAP \qquad (2.6.2)$$

where S is the charge sensitivity in pC/N

A is the area of the surface

P is the applied pressure

With these two governing equations, the output voltage from a given pressure can be determined. Single crystal quartz is the most stable and is nearly loss free mechanically and electrically. Therefore, it is a very popular piezoelectric material. Barium titanate is

an artificial piezoelectric ceramic material that is more economical than quartz and has a much higher sensitivity. While the material is held above the Curie temperature of 125°C, it is polarized by applying a high voltage to the material. The polarization is held while the barium titanate is cooled, and the piezoelectric effects become permanent. Lead Zirconate Titanate (PZT) is another widely used piezoelectric ceramic. It is often used as a driver in ultrasonics. Piezoelectric materials used as sensors of ultrasonic waves have very high frequency responses in the MHz range.

2.7 Q-Switching:

The process of creating a very short time duration of the pulse is done by Q-switching. This leads to much higher peak power values for the pulse than would be attained without the Q-switching. Q is the quality factor for a laser that measures the internal loss of energy within the laser cavity. The higher the Q the lower the loss, and a high loss cavity can store more energy than a low loss. The basic principle is to block the laser cavity while still pumping the laser medium with energy. The population inversion can get very large, but the light is unable to oscillate because it can't reflect between the two mirrors. For this research the Q-switching was performed with a Pockel cell. It is possible with electronics to created multiple pulsing during a single flashlamp cycle of the laser. (10) Studies have been done to investigate the possibility of reducing the system bandwidth and improving the signal to noise ratio by repetitive Q-switching. For the purpose of this experiment, a single shot laser was used which produced a single Q-switched pulse of laser light.

Chapter 3

Ablative Laser Ultrasonics Experiments

3.1 Experiment:

The experimental setup of figure 3.1.1 was calibrated, and then used on an Aluminum plate and a Ti alloy tube. The calibration consisted of two parts, measurement of energy per pulse, and pulse duration. These two parameters must be known and measured experimentally in order to calculate the energy density imparted to the surface and the peak power experienced by the surface. In order to measure the pulse duration, a photodiode sensor and beam splitters were added. The photodiode also allowed for a more accurate trigger than was used previously. In earlier work, the oscilloscope had been triggered by a 30 volt pulse coming 200 to 300μs ahead of the laser shot. The exact timing of the trigger system was not known, making it difficult to precisely measure the arrival time when the first dilatational waves to reach the piezoelectric sensor.

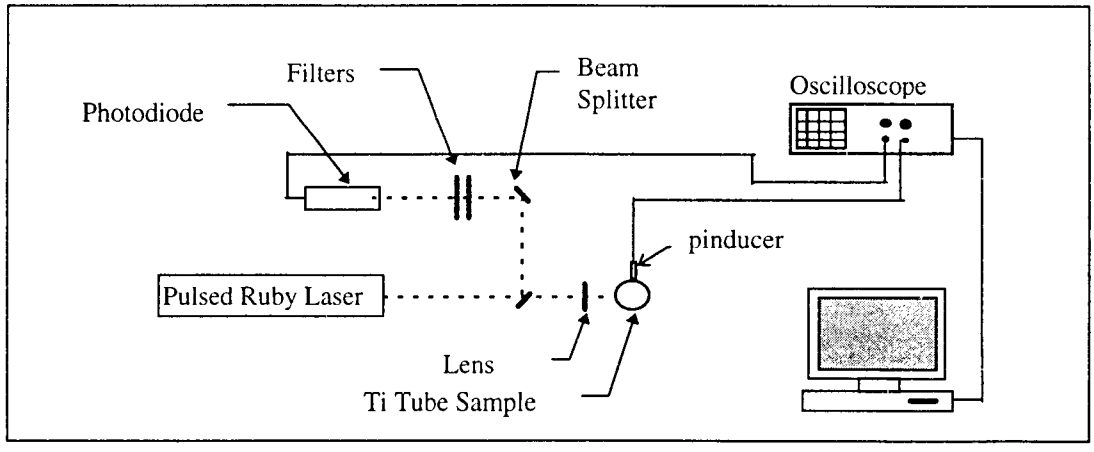

Figure 5. Experimental Configuration

The transient data from the pinducer was collected with a digital 4420 Techtronics oscilloscope with a 500 MHz bandwidth. The pinducers were manufactured by Valpey Fisher using a pinducer with a 2 MHz bandwidth crystal. The pinducer is the limiting factor in the bandwidth of the signals that can be received. The Holobeam ruby laser produces visible red light of 694 nm wavelength. The light was focused on the sample with a variety of lenses. The ruby laser pulse was Q-switched to provide a very short intense burst of light on the surface.

In order to protect the photodiode from the intense burst of laser energy, two beam splitters and numerous filters were used. These were glass slides held at a 45° angle. For a glass slide, the reflectance varies with the polarization and angle of incidence with respect to the glass slide. For the energy calculations a reflectance of 4% was chosen. If the light were polarized perpendicular to the plane of incidence of a 45° glass slide the reflectance could be as high as 8%.

3.2 Calibration:

Properties of the laser pulse must be investigated prior to collecting results with a laser instrument. The pulse energy, duration, and profile all must be known. The laser deposition energy was measured with a Scientech 38-01010 Disc Calorimeter designed for measuring Q-switched pulsed laser output. The energy density imparted with a direct shot from the ruby laser would be too high for the calorimeter without using a beam splitter to measure the energy. Permanent damage of the calorimeter was avoided by using a beam splitter to ensure that a maximum of 4% of the energy in the laser beam reached the calorimeter surface. Figure 6. shows the experimental setup for the measurement of the pulse energy.

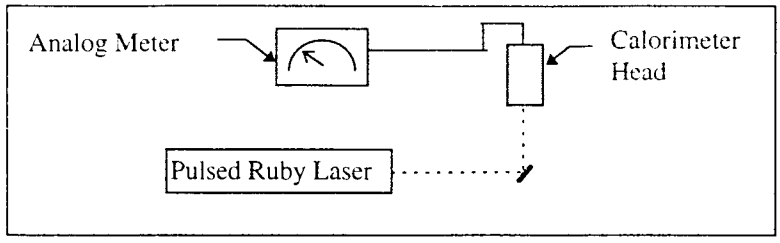

Figure 6. Pulse Energy Measurement Setup

The calorimeter has a 12 second time constant so the meter had to be given time to stabilize. All lights in the room were turned out to reduce the amount of error in the measurements. The calorimeter is sensitive to heat from fingers, light, air currents in the room. At higher energy densities the air currents are not as critical. Several measurements were taken to verify the repeatability of the experiment. One glass slide was used to decrease the maximum energy density that the calorimeter head would receive. Based on a glass slide reflectance of 4%, the laser was depositing approximately 2 Joules of energy on the surface. Error is introduced if the glass slide reflectance is not exactly 4% or if the angle is not exactly 45 degrees. Error is also introduced from stray light sources, even that coming under the door with the lights out. For a single shot 0.08J was measured at the calorimeter head. The conversion for the glass slide reflectance then yields the total amount of energy that was deposited on the surface. Equation 3.2.1 is the simple equation to calculate the total energy per pulse. The numerator values are the energies in Joules, J, and the denominators are the percents of energy converted into decimal form. By solving for the unknown energy X, this gives the energy if 100% of the beam were directed at the photodiode. This relationship assumes the energy absorbed is a linear function of the energy incident on the calorimeter head surface.

$$\frac{0.08J}{0.04} = \frac{XJ}{1.00} \qquad (3.2.1)$$

With the change in apparatus to the photodiode triggering system the exact time when the light hits the surface is measured within a few nanoseconds. This method eliminated the error involved in determining when the laser energy was deposited on the surface. The change of apparatus also aided in reducing the amount of noise apparent in the signal when the laser was fired. In some instances there was no noise at all collected when the laser was fired and the first signal is the arrival of the dilatational P wave. Before the changes there was always a very large noise spike when the laser was fired. The changes led to significant improvement in the experimental setup.

The photodiode was set up and used in the manner shown in the schematic diagram figure 5. In order to cut down the intensity of the signal five cross polarized filters were used in conjunction with the two beam splitters. This allowed for a signal in the 200mV range from the photodiode, yet preserving the integrity of the light pulse signal from the laser. The photodiode has a 1 ns response time, which is fast enough to accurately portray the profile of a 20 to 100 ns pulse. Figure 7. is a graphical representation of an actual pulse profile showing the full width half height ,FWHH, of the pulse profile.

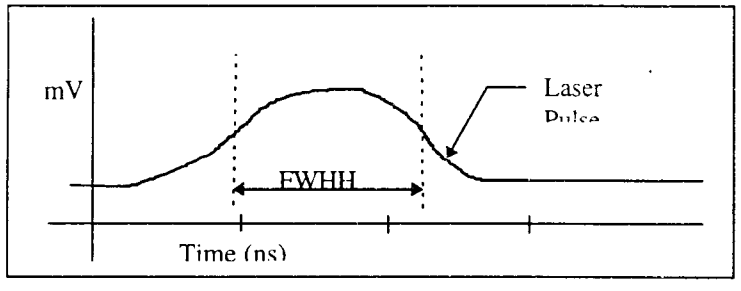

Figure 7. Q-Switched Ruby Pulse Profile

The profile resembles a Gaussian distribution. The beam profile is affected by the way in which the laser cavity is designed. The photodiode was manufactured by Thor and under peak illumination has a maximum trigger voltage of 22.5 Volts The laser pulse

typically had a FWHH value of approximately 70ns. The actual amplitude of the signal depended on the type and number of filters applied. Once all the properties of the laser being used were found then data could be collected for particular cases.

3.3 Al Plate Test:

A flat Aluminum plate was used to test the apparatus for ultrasonic signals. Through transmission mode was used, in which the piezoelectric sensor was on one side of the plate and the laser pulse deposition was on the other side of the plate. A diagram of the schematic for this is shown in figure 8. The plate was 12 inches wide by 9 inches high. By having a plate that was much wider and taller than the distance of signal propagation, the edge effects would be decreased. This makes the interpretation of the ultrasonic signals less difficult.

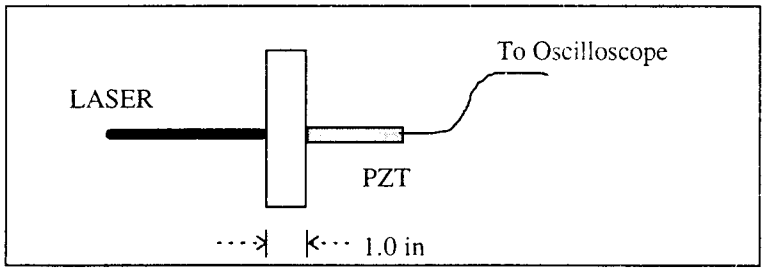

Figure 8. Al Plate Setup Using Pinducer

The aluminum plate was 6061T6 type alloy, and the nominal plate thickness was 1.00 inches. A couple of drops of oil were used as a couplant at the pinducer and metal interface. A black marker was used to increase the adsorption of the laser energy by the metallic surface. The generation of sound waves requires a transient heat source at the surface so it was important to maximize the energy adsorbed. The laser was focused with a plano-concave lens to an area of approximately 32 mm^2. The unfocused ruby laser had

a beam area of about 72 mm^2. It was found through experimentation that slight focusing of the original beam provided excellent signals at the pinducer. The sample was positioned approximately one meter in front of the laser, and the area of the beam was measured from burn patterns produced on polaroid film. The experimentation produced strong dilatational waves which resulted in a strong initial wave arriving approximately 4 μs after the laser pulse. Then repeated echoes were seen at 8 μs intervals. This is what was expected experimentally. Figure 9. is the test data from the aluminum plate.

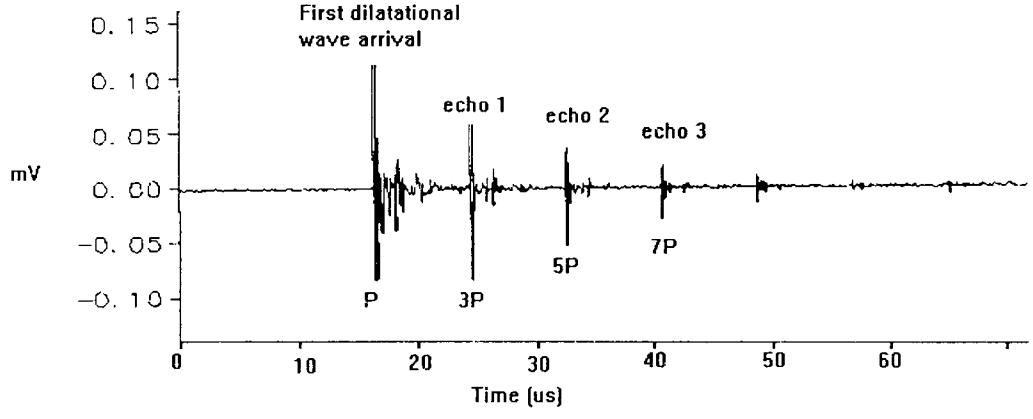

Figure 9. Laser Induced Longitudinal Wave with Echos in Al 6061T sample

The data showed the initial dilatational wave or P wave followed by mode converted shear waves and then the first echo or 3P wave arrives. The mode converted shear waves are the smaller set of waves that are trailing the large dilatational echoes. Shear waves produced from the initial laser shot strike the back wall and convert to longitudinal waves which were measured by the pinducer. The amplitude decreases due to attenuation of the sound wave in the aluminum medium. The pinducer and couplant are insensitive to shear waves, because the couplant is a medium density oil. When the ablation occurred dilatational, shear, and surface waves were generated simultaneously. The large echos

that can be seen on the right hand side of the trace are 5P, 7P, 9P, etc pulses. The pulses begin to diminish as they are attenuated within the medium. The initial laser impulse occurred 4μs before the first arrival. No surface waves arrived during the sampled time window due to the large distance they would have to travel around the entire boundary of the plate to arrive at the pinducer. By knowing the thickness of the plate and the time between echoes the velocity of the dilatational pulses in this aluminum alloy can be determined experimentally. The experimental longitudinal velocity of aluminum in this sample was measured to be 6280 +/- 80 m/s. The plate thickness was 1.001 +/- 0.001 and an echo transit time of 8.1 +/- 0.1 μs was measured. The published value for the longitudinal velocity of aluminum is reported to be 6320 m/s (5). Thus, the experimental value and the published value were in the same range when experimental error was accounted for. These results verify that the experimental setup was working and the data was valid for this test case.

A Power Spectral Density (PSD) analysis of the signal was performed to determine the frequency content of the induced sound pulses in the aluminum sample. The power spectral density is equal to the mean-square spectral density times the quantity π. The mean square spectral density is calculated by taking a narrow band filter and applying it to the data. The amplitude of the signal that is within that band width is squared and divided by the bandwidth. The narrow band filter is then moved an increment Δw and the squaring process is repeated. The mean square spectral density, ϕ(w) is represented by the following formula. [23]

$$\phi(w) = \frac{\overline{V_{i.w}^2}}{\Delta w}. \qquad (3.3.1)$$

where w is the frequency

Δw is the bandwith of the region

$V_i(t)$ is the voltage of the signal recorded

This results in a graph that is proportional to the amount of a given frequency contained in the signal. Thus this method is useful for determining what frequency of signal dominates in the aluminum plate when the laser energy is deposited on the sample.

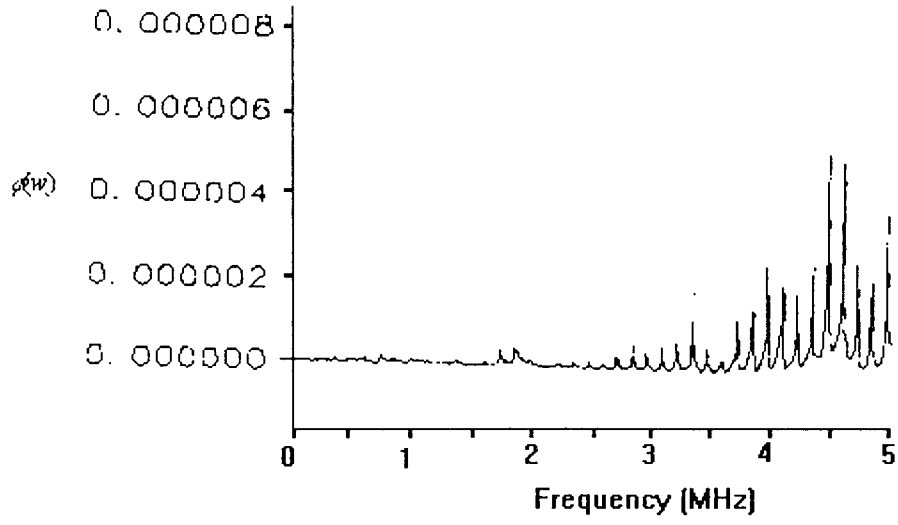

Figure 10. PSD of Al Plate data

The results of figure 10. show small spikes at 1.7 and 1.8 Mhz, followed by another spike at 3.3 MHz. The most dominant frequencies occurred at 4.4,4.5 and 4.9 MHz. This showed that a band of frequencies in the 4 to 5 MHz range was formed when ultrasonic waves were induced by the laser. The bandwidth of ultrasonic pulses that were produced was highly dependent on the shape of the laser pulse and the pulse duration. The shape of the pulse can be changed by alterations in the laser cavity, and the time duration of the pulse can be controlled by the Pockel's cell operation. The attenuation is a function of the frequency. The wavelength of the penetrating ultrasonic signals provide useful information. Like X-rays, the resolution is dependent on the wavelength. The higher

frequency waves with small wavelengths provide good resolution, however they attenuate faster in the medium so a compromise has to be reached.

3.4 Ti Tube Sample:

The second sample that was tested was a Ti tube. The tube was clamped at one end and the area two inches in from the free end was used for testing. Figure 11. shows the experimental setup for this case. The laser energy was focused to an area of 25 mm^2. A variety of areas were tested for strength of longitudinal signals and this one seemed to produce good signal amplitude. The focusing was performed in the same manner as the Al plate with a plano-convex lens. The area was determined by measuring the burn pattern on a polaroid film.

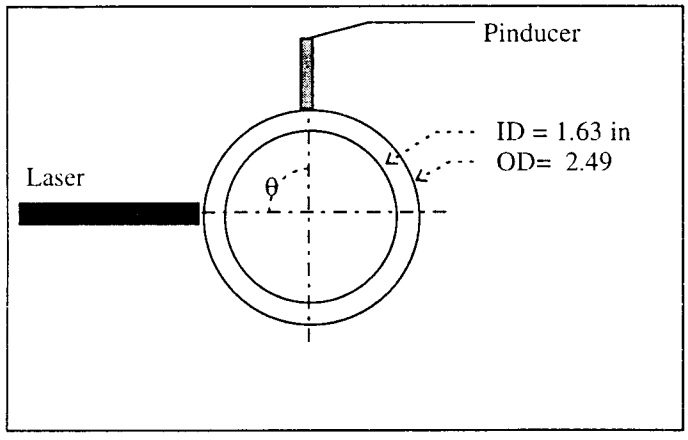

Figure 11. Ti Tube Arrangement Using Pinducer

The laser energy was deposited on the side of the tube. The tube was 6.42" long with a cross sectional area as shown. The angle of the pinducer with respect to the laser was changed to observe the effects of angular displacement. In one particular experiment the initial angle was 10°. The pinducer was then successively incremented to 20°, 30° , and

40°, and the waveforms were captured. Figure 12 is the result of that particular experimental arrangement.

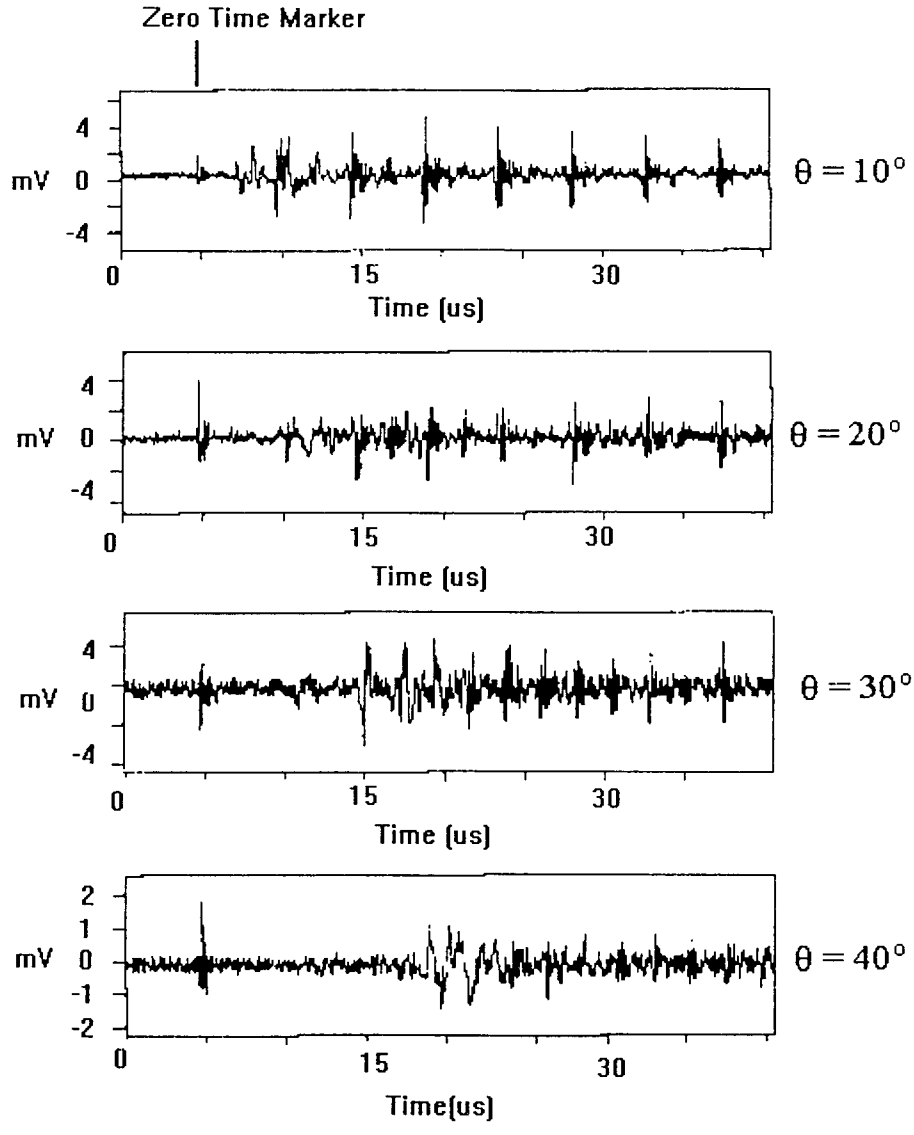

Figure 12. Ti Tube Data

From the 10° data it can be seen that there is a lower frequency component that arrives first. This is the Rayleigh surface wave. The amplitude is quite large. The spike on

the left that is the same for each of the four graphs is the zero time fiducial marker for the laser. This is the moment that the laser is fired as indicated by the electromagnetic spike in the signal. The trend that stands out in the data is that as the pinducer is moved angularly around the sample, the ultrasonic waves take longer to reach the pinducer and thus the signal moves towards the right.

Figure 13. shows the Rayleigh wave and the dilatational pulses quite clearly. Note the Rayleigh wave is superimposed over dilatational waves in the beginning, and then the pinducer sensor only sees repetitive dilatational pulses. The smaller signals in between the pulses can be attributed to mode conversion, and interference effects in the hollow cylinder. The dilatational pulses, D1, D2, D3, and D4 can be explained by geometric spreading and the boundary effects of a spherical sound pressure wave impinging on a cylindrical surface.

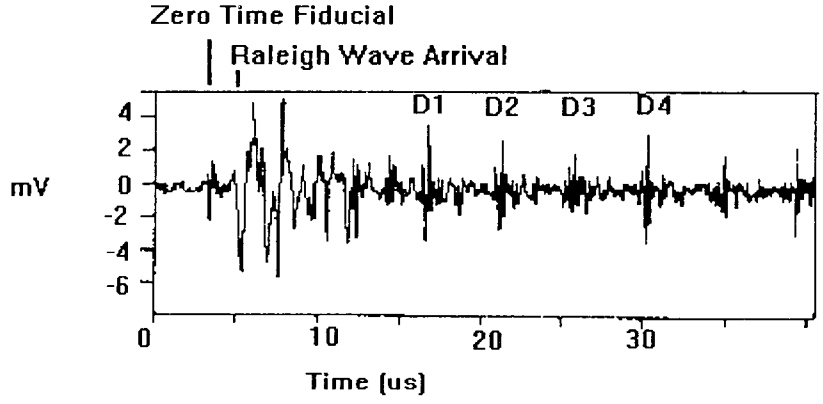

Figure 13. Rayleigh Wave Example for Ti Tube

When a sound wave impinges on a curved surface, the surface acts like a lens, focusing the sound to a focal length prescribed by the geometric conditions. The standard lens diagram can help to visualize the situation. In the solid tube the effects are now in three dimensions instead of two, but the basic idea is the same. The laser impinges on the left side of figure 13, and the sound then propagates across the medium and geometrically

spreads as it does so. The sound along the center of the surfaces will echo back and forth, as it is largely unaffected by the lens effect. As the sound bounces back and forth it geometrically spreads outward. The waves that are spread outward are then susceptible to the lens effect and they propagate in the directions of the two diagonal arrows in the diagram. This is an explanation for amplitude of the repetitive dilatational signals D1, D2 and so on which does not decay exponentially. The times between the dilatational pulses are almost identical. This time spacing indicates that the waves are traveling along diagonal path lengths. The amplitude of the signals goes by an inverse square law of the distance from the source. Since the amplitudes of all the repetitive pulses are similar this would tend to indicate that the waves are traveling along the same path, and that they are being generated by a common source such as the echoes along the centerline in figure 14. As the sound echoes along the centerline, it spreads out geometrically and then it is affected by the lens curvature. The direction of propagation changes accordingly.

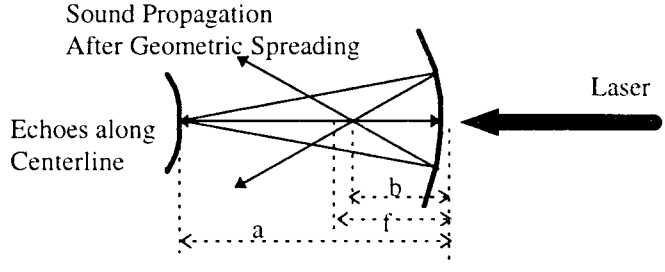

Figure 14. Tubular Reflections Occurring Due to Lens Effects

A power spectral density analysis was also performed on the Ti Tube data to see what frequencies dominated in the tube when laser ultrasonics was applied. Figure 15. is the PSD for the Ti Tube. Conventional utrasonic inspection uses frequencies between 2 an 5 MHz except in special circumstances, such as large attenuation due to grain size. For each material that is being inspected, one must determine if the pulse duration is producing ultrasonic waves that will allow the defects in that object to be discovered by nondestructive evaluation.

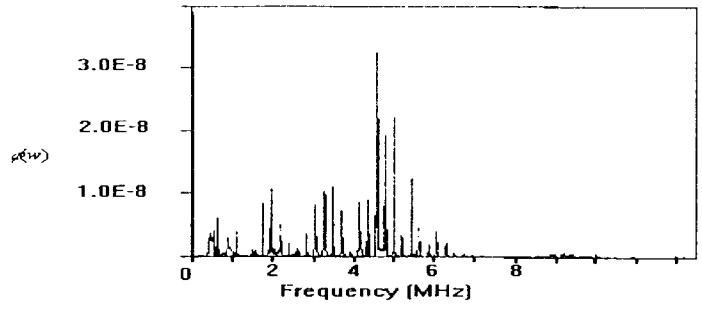

Figure 15. PSD for Ti Tube

For the PSD shown in Figure 15., the main frequency spikes occur at 4.59 MHz, 4.79 MHz, 5.01 MHz. These results indicate that the pulse duration of approximately 70ns is acceptable for ultrasonic inspection of defects. If the results had been different, the type of Pockel's cell used could be changed to vary the pulse duration and the resulting frequencies to be of a range that would be useful for evaluation.

Chapter 4

Weld Inspection

4.1 Weld Discontinuities

A weld contains discontinuities that can lead to failure of the weld if the stresses caused as a result of those discontinuities exceed the yield strength of the material. The application of heat and the fusion of the metal results in stresses of high magnitude from thermal expansion and contraction of the weld metal during solidification. The thermal stresses remain after cooling and can cause distortion. Discontinuities create stress concentrations in the metal. A common discontinuity is porosity due to dirt, rust, moisture on the surface base metal. Another discontinuity is slag inclusions which are oxides and non-metallic solids entrapped in weld metal. Generally slag rises to the surface due to lower specific gravity, but sometimes it gets trapped in the weld. Tungsten can also become included in the weld when the electrode is touched to the liquefied metal if tungsten inert gas (TIG) welding is used.

Incomplete fusion can cause weld failure as well. Incomplete fusion can occur when the base metal fails to be raised to the melting point. Another cause of incomplete fusion is failure to dissolve the oxides on the surface. Inadequate joint penetration occurs when the filler metal fails to completely fill the root of the weld largely due to heat transfer conditions. An example of this is when the sides of the weld reach the melting point before the bottom, so the sides fuse together yet the bottom never reaches the melting point. Two main orientations of cracks also appear as discontinuities in welds. Transverse base metal cracks can occur across the direction of welding steels of high hardness. Longitudinal base metal cracks can also occur. They often result from high hardness and low ductility in the heat affected area of the weld. The rate of cooling, thermal properties of the base metal, the temperature produced by the weld process, and the ambient temperature are all factors that effect the formation of transverse and

longitudinal cracks in the weld material.[36] All of these types of discontinuities that appear in welds are detectable with ultrasonic pulses.

4.2 Conventional Ultrasonic Weld Inspection:

The need for the inspection of welds is driven by economics in industry. The primary desire is to evaluate the effects of discontinuities on the structural integrity of the weld. In a 500MW fossil fuel electric power plant 10% of the cost of construction is welding alone, and welding comprises 20% of the maintenance costs. Failure of a pipe due to dissimilar metal weldment can cause plant shutdown and costs approaching one million dollars, and this is assuming there was no loss of life due to the failure.[31] The industrial need is there for a method to evaluate welds for discontinuities that can cause failure of the weld. Using ultrasonics to inspect welds has been used to locate porosity, slag inclusions, lack of side wall fusion, lack of inter-run fusion, lack of root penetration, undercutting and cracking. Transverse waves are most commonly used for weld testing. At critical angles of 33 degrees in steel and 30 degrees in aluminum, the transverse waves totally reflect internally. This allows them to travel greater distances and only attenuation and geometric spreading dissipate them. A common conventional probe for testing is the 70 degree probe at 4 MHz. Frequencies between 2 and 5 MHz are most commonly used for testing. Techniques which move the pulse-echo transducer from one half to one full skip distance, S, are used to move the ultrasonic beam up and down the weld/plate interface. Other geometric patterns can be use multiple transducers for specific cases. Figure 16 shows the transducer on the left. Then to scan the weld, the transducer is shifted along the weld to the position of the dotted transducer. As the transducer is moved along, the acoustic waves scan the side of the weld. The picture on the far right of figure 16 shows how the angle theta is defined with respect to the metal surface.

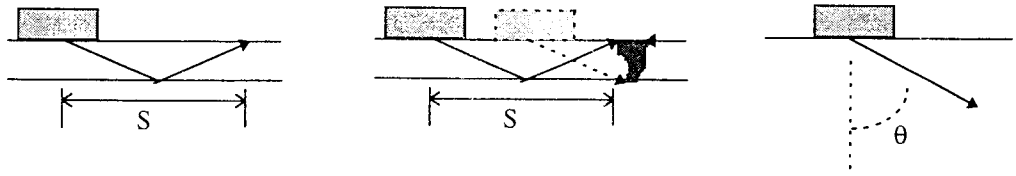

Figure 16. Ultrasonic Beam Propagation Using Transverse Waves

Since the ultrasonic pulse generated by a laser is always perpendicular to the point of application of the laser, laser pulses are under the zero degree category for beam propagation angles. In the ablation mode the longitudinal wave is emphasized.
By using fiber optics and phased arrays, laser ultrasound can be directionally controlled. Thus lasers are not only limited to the zero degree category. This is important because often in weld inspection the welds are inspected from the side as the diagrams above indicate.

4.3 Applications for Laser Ultrasonics to Weld Inspection

Several researchers have looked into the idea of evaluating weld quality by the use of laser ultrasonic systems. These systems are ideal because the area around a weld is often at high temperatures and coupling of traditional transducers becomes difficult. Two approaches are used. One approach is the development of an on line control system to assist in identifying defects as they form and change weld settings and geometry to alleviate the defects during welding. Another approach is the identification of the defects in the weld after the weld has been completed. Dewhurst [30] and Scruby [28] both looked at identifying a crack in a completed angled butt weld section. The type of crack that was analyzed typically forms in butt welds in the heat affected zone just outside the area that was welded.[5] Finely distributed slag inclusions are generally attributed to the cause of this type of defect. Figure 17. shows the experimental setup for clarity.

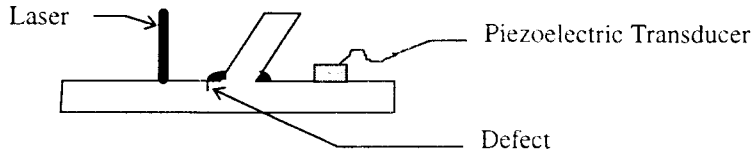

Figure 17. Scan Apparatus [28]

The piezoelectric receiver was an angled perspex shoe. The data clearly showed the echo from the crack tip reflecting the compression wave. The method of using laser-generated Rayleigh waves to detect surface cracks has proven very accurate and the results from the study of the angled butt weld were successful.[28] Dewhurst looked at the same geometric setup with a Electromagnetic Transducer (EMT) instead of the piezoelectric sensor in the diagram above. The results using the EMT were also successful.[30] Both researchers found that cracks in the heat affected zone can be detected by observing Rayleigh wave echoes. Thus one type of weld discontinuity has been identified and methods have been developed to search for that type of discontinuity.

Another experiment in weld analysis was performed in on a steel bar that was blind side welded to a steel plate. The sample weld was examined with laser ultrasonics. Through transmission mode was used in which the laser was focused on one side of the weld and a pinducer was on the opposite side of the sample. The amplitude of the utrasonic signals was compared for various positions along the weld. [20] It was concluded that higher quality welds led to lower attenuation of the signal. This was an indication of the amount of slag inclusions and porosity in the weld sample. This research was looking for a general way to categorize flaws in a weld sample.

In terms of on line monitoring of weld quality, research has been done to look into this possibility. The goal was to be able to detect defects as they are forming in the weld material by monitoring the solid/liquid metal interface and by using the laser input in a control system to change the welding voltage, arc length, or speed accordingly. In order to be used in a control process, the monitoring must be done in the first few fractions of a second of the welding process.[32] A Nd:YAG laser was used to monitor the signals in a

weld pool just before welding, and during welding. The signals changed, but the reasons for all of the signal changes were not discovered. There are many factors which can effect the transmission of sound through a weld pool, such as the temperature gradients, mode conversion, the motion of the pool surface, and the shape of the solid/liquid metal interface.[29] An experiment was set up in which some of the variables were taken out by using glycerin to model the molten metal. The glycerin was placed in predetermined geometric pools, and ray tracing was used to predict the resulting signals that would be seen at the piezoelectric sensor. The number of factors that influence the behavior of the sound field make it extremely difficult to predict what the signal should look like.

In order to understand what is happening with laser ultrasonics, the variation of an ultrasonic field due to temperature gradients must be known. The ultrasonic sound field is dependent on temperature changes, so this can lead to errors in determining the position of a discontinuity. When a sound field enters a hot area it slows down. This increases the transit times which causes error in positioning. Determining the magnitude of this error is crucial to the accuracy of the ultrasonic inspection. A semi-infinite weld is modeled as a half cylinder in an block of much larger volume. The temperature across the weld was attained using Green's function and integrating this over the area of the weld. The temperature distribution was used to determine the variation in the elastic constants over the weld area. This is an idealized model because the weld properties are taken to be independent of temperature and the thermal properties of the pool are assumed to be homogenous. Austenitic steel and iron were modeled. Ray tracing was used to determine the transit times of signals reaching the weld pool . This research showed that if the high temperature dependence of the elastic constants is known, then it is possible to use ultrasonics to monitor a weld interface location to within 0.5mm.[32] In practice, the experimental errors are slightly larger than this, and this can be due to anisotropy and thermal expansion which are not accounted for in the theoretical model. The author determined that the errors for shear waves in the medium were twice those for longitudinal waves which is an advantage for ablative utltrasonics which produces strong longitudinal waves.

Weld studies with conventional ultrasonics can provide insight to how the ultasonic systems should be designed and applied. An experiment was set up with a 45 degree longitudinal transducer that was mounted to send sound into a single beveled V groove weld. The output was used to determine characteristic acoustic signatures from incomplete sidewall fusion, gross porosity, and undercut. Once the characteristic signatures have been discovered then they can be integrated into the welding control system. The conditions to generate each of the desired discontinuities were determined as a function of variable welding parameters such as electrode height, position, speed, gas content, etc. By varying these conditions defects could be generated. The defects were then substantiated by destructive evaluation and micrographs of the welds at precise transducer locations. Ray tracing was used to determine the signal content that was captured at each transducer location. The authors showed that each type of defect yields a signature that can be broken down into components by ray tracing.[33] A system needs to be developed that recognizes these signals and compensates for them by changing weld parameters. This system has yet to be developed. Since the maintenance of coupling uniformity is difficult with gels, the laser systems seem to be ideally suited.

A different system has been developed to scan welds as soon as the weld has been created.[34] Two types of defects were created, lack of fusion and porosity. Lack of fusion was created by reducing the weld current and mistracking the weld head to one side. Porosity was instilled in the samples by reducing the gas shield flow rate. Flaws were confirmed with radiography or destructive evaluation. The system developed used a piezoelectric transducer and pattern recognition to determine if a flaw existed. Roughly 90% of the flaws were detected. This system had difficulty distinguishing between types of flaws even though it successfully identified whether a flaw existed at that location. The type of weld that was scanned is shown in figure 18.

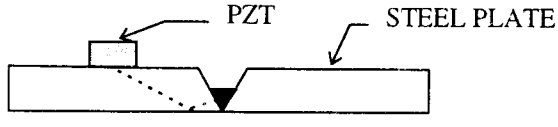

Figure 18. Weld For Pattern Recognition Testing

The lack-of-fusion flaws returned signals of higher amplitudes than that from the porosity signals and was reported to be generally a replica of the original waveform from the transducer. The porosity signals generally consisted of several reflections which resulted in many cycles in the waveform. The method was designed to detect flaws in a multiple pass weld before they were covered up by the next pass. The next step is to design and test a commercial system, and the authors believe that this is feasible. [34] As of yet, purely LBU systems have not been applied to the scanning of welds to determine their flaw type and content.

Chapter 5

Conclusions and Recommendations

5.1 Conclusions:

5.1.1 *Ti Tube*:

Signal interpretation is difficult for complex geometries such as a Ti tube. A possible explanation was proposed to explain the signals that were attained through experimentation. This is a simple explanation founded on the transit times of the dilatational pulses that were seen in the output. In order to have such an even spacing, there must be a simple geometry driven oscillation causing the reflections. Many challenges were overcome during this project. Many of the problems became evident when the system was checked for laser pulse shape and duration and pulse energy output. These are the preliminary calibration tests were done before the data was taken. The Pockel's cell was producing double pulses which was later attributed to flaws in the Pockel's cell. A coaxial cable broke underneath the shielding, so that from the outside the cable looked fine. Noise in the signals led to detecting the problem. A fast photodiode triggering system was added which decreased the background noise when the laser was fired. Laser energy measurements were taken to verify that the energy imparted to the surface was indeed enough to classify the system as one that would cause ablation of the surface and plasma formation. The laser system is in much better condition now than it was when the experimentation began. Thus, this is a notable improvement.

It would be possible to detect flaws in a Ti tube in a manner similar to the scanning of composite hat sections for defects. With a laser based ultrasonic unit this would be an ideal method of finding flaws hidden within the tubes. If the laser were used to obtain data for many points, a three dimensional map of the hidden flaws could be created. While the cost of these systems is fairly high at the moment, it is believed that they could be used reliably to evaluate the defects in tubes.

5.1.2 *Large Butt Welded Plates*:

For the purposes of the inspection of large welded structures further research needs to be done. Since conventional ultrasonics uses transverse waves at high angles, the application of laser ultrasonics can not be based solely on conventional ultrasonic research. A literature survey was completed and resulted in little research on scanning a laser system over a weld to identify defects. Zero degree probes induce signals perpendicular to the surface, similar to LBU. Zero degree probes are seldom used in conventional ultrasonic weld inspection because coupling a transducer to a weld area poses problems of coupling thickness, reflections in the coupling layer, and orientation and direction of induced signals. However, a laser can be focused on the top of the weld without heed to many of the problems that face a transducer system. With the advances of fiber optic cables, the laser and interferometer assemblies can be 10 meters away from the inspection area with cables running to the area. The sensitive laser equipment does not have to be located in the area immediately next to the test area.

For the purpose of inspecting large butt welds the laser may in fact be the ideal choice. The grain structure of the weld can pose problems in the evaluation of the ultrasonic signals. A course grain boundary provides surfaces that scatter and disperse acoustic energy. These reflections can cause difficulty in signal evaluation. Certain types of welds pose more problems than others, so the weld type that is of interest needs to be evaluated. The only way to know for sure if laser systems can be applied is to get some samples that have realistic defects in them. The defects can be generated by changing the input parameters on the welder. This includes, alignment, heat input, rate of feed of the wire, gas composition, etc. Then the laser system needs to be applied to scan for the known defects. The weld samples need to be destructively evaluated and microscopy applied to determine the exact location and type of defect involved. This is the path that composites have followed. Researchers have imbedded known defects at known positions and have found them successfully. This method needs to be applied to laser ultrasonic

weld inspection. The technology is there, but it has not been applied extensively to the evaluation of welds.

5.1.3 *Future Research Recommendations*:

The next step is to take an LBU system and collect and analyze data that comes from known defects in a welded sample. In order to be used extensively in industry the LBU systems are the ideal method. In this manner, the sample surface never has to be contacted with a piezoelectric sensor. Couplant does not have to be used for the laser systems, so the surface is not contaminated. Advancements have been made in discriminating between light gathering fluctuations and ultrasonic signal intensity fluctuations, and these advancements have overcome at least one of the challenges in the use of laser ultrasound. One author applied a pattern recognition system that did find flaws, but did not determine what type effectively. This type of a system needs to be developed for weld analysis, only one that is more accurate than the one previously developed. If one type of inhomogeneous material such as a multilayered composite, can be scanned for flaws then the premise is there for the scanning of other inhomogenous materials such as a weld area.

Research should focus on the weld after creation, because this case does not have to take into account the thermal stratification of the weld, and the variations of the elastic constants of the material due to that thermal stratification. It is possible to generate laser ultrasound in a non zero degree direction by the use of phased arrays and time delay of the laser signals. If this technology proves reliable, then laser systems can replace the ultrasonic evaluations that are currently available. Another idea is to find a method of causing the laser ultrasound to be bent to angles by using refraction or some other technique. If this challenge can be overcome then the laser systems could do the same work as the conventional systems without coupling affecting the results. The promise is there for complete LBU inspection of welds, it just needs to be investigated further with more experimentation.

Bibliography

1. Hecht, Jeff. *Understanding Lasers An Entry Level Guide*. Indianapolis, Ind: H.W. Sams, 1988.

2. Scruby, C.B., and L.E. Drain, *Laser-Ultrasonics: Techniques and Applications* (Adam Hilger, Bristol, UK, 1990.

3.Monchalin, Jean-Pierre. *Review of Progress in Quantitative Nondestructive Evaluation,* vol 12. edited by D.O. Thompson and D.E. chimente, Plentium Press, New York, 1993 p.495.

4.Kolsky, H. . *Stress Waves in Solids*, New York, Dover Publications, Inc., 1963.

5.Krautkramer, J. and H. Krautkramer. *Ultrasonic Testing of Materials 4th Edition.* Berlin, Springer-Verlag, 1990.

6.Hrovatin, Rok.. *Effect of Plasma Shielding in laser ultrasonics Optoacoustic characterization.* J. Appl. Physics, Vol 75, No. 12. June 1994, .pp8207-8209.

7.McKie, Andrew *Practical Considerations for the Rapid Inspection of Composite Materials using Laser-based Ultrasound.* Ultrasonics, Vol 32, Iss 5, 1994, pp 333-345.

8. Cawley, P *The Rapid Non-destructive Inspection of Large Composite Structures* Composites, Vol 25, Iss 5,1994, pp 351-357.

9. Dewhurst, Richard J. *Defect Visualization in Carbon Fiber Composite Using Laser Based Ultrasound* Materials Evaluation, August 1993, pp. 935-940.

10. Wagner, James W. Generation of Ultrasound by Repetitively Q-switching a pulsed Nd:YAG laser. Applied Optics Vol 27. No 22. 15 Nov 1988, pp 4696-4700.

11. Melles Griot Inc. *Optics Guide 5* Irvine, CA, 1990, pp. 5-23, 11-3.

12. Bayon, A. *Determination of the Elastic Constants of Isotropic Solids by Optical Heterodyne Interferometry*. Journal of Acoustic Society of America. 96 (4) Oct 1994 pp. 2589-2592

13. Noui. L *A Laser Beam Deflection Technique for the Qualitative Detection of Ultrasonic Lamb Waves*. Ultrasonics. Vol 31, No 6, 1993, pp. 425-431.

14. Schindel, D. W. *High-Temperature Pulsed Photoacoustic Studies of Surface Waves on Solids*. Journal of Acoustic Society of America. Vol 95. No 5 Pt. 1, May 1994, pp. 2517-2524.

15. Scruby. C.B. *Quantitative Studies of Thermally Generated Elastic Waves in Laser-irradiated metals* J. Appl. Phys. 51912), Dec 1980, pp. 6210-6216.

16. Dewhurst. R. J. Edwards A. D. *A Remote Laser System for Ultrasonic Velocity Measurement at High Temperatures* J. Appl. Phys. 63(4) Feb 1988, pp. 1225-1227.

17. Piche, L. Champagne. B, J-P Monchalin *Laser Ultrasonics Measurement of Elastic Constants of Composites* Materials Evaluation 45 Jan Feb 1987, pp. 74-79.

18. Schreiber, E. , O. Anderson, and N. Soga, *Elastic Constants and Their Measurement* McGraw Hill, New York, NY, 1973.

19. R.M. White *Generation of Elastic Waves by Transient Surface Heating* J. Appl. Phys 34 3559 1963, pp. 3559-3567.

20. Calder. C Wen, Jisheng. *Ablative Laser Ultrasonics Applied to As-Cast Surfaces* Proceedings, 1995 Spring Conference Society for Experimental Mechanics (SEM) Grand Rapids, Michigan June 1995 pp 603-608.

21. Calder. C. Park, Heeyong *Laser Ultrasonics for Large Metal Structures* Proceedings, Seventh World Conference on Titanium, San Diego, July 1992.

22. Lai W. Michael, Rubin David, Erhard Krempl *Continuum Mechanics* New York, 1993

23. Doeblin, Ernest O. *Fourth Edition Measurement Systems Applications and Design* US, McGraw-Hill, Inc 1990

24. Burger C.P., Smith J.A., Rathe U.W. *Lasers With Optical Feedback as Displacement Sensors.* Optical Engineering Vol 34, Iss 9, 1995, pp 2802-2810

25. Dewhurst R.J., Williams B.A. *Differential Fiber Optic Sensing of Laser Generated Ultrasound* Electronics Letters, Vol 31, No. 5, 1995, pp 391-392

26. Duggal A.R., Yakymyshyn C.P *Optical Detection of Ultrasound Using a Microchip Laser.* Rev. Sci. Instrum., Vol 66, No. 8, 1995, pp 4102-4113

27. Nishino H., Tsukahara Y, Nagata Y, Koda T., Yamanaka K. *Optical Probe Detection of High-Frequency Surface Acoustic Waves Generated by Phase Velocity Scanning of Laser Interference Fringes* Japanese Journal of Applied Physics, Vol 33,No. 5B, 1994, pp 3260-3264.

28. Scruby, C.B. *Some Applications of Laser Ultrasound* Ultrasonics, Vol 27 July, 1989, pp 195-209

29. Carlson N.M, Johnson, J.A. *Laser Sound Generation in a Weld Pool* Review of Progress in Quantitative NDE vol 7B, 1987, pp1485-1494.

30. Dewhurst, RJ *Noncontact Detection of Surface-breaking Cracks Using a Laser Acoustic Source and an Electromagnetic Acoustic Receiver* Applied Physics Letters , Vol 49, 1986, pp 374-375.

31. Keefer D.W., Reuter W.G, Smartt H.B, Johnson J.A, David S.A., *Needed- Verified Models to Predict the Fracture of Weldments* Welding Journal, Vol 72, Iss 9,1993, pp 73-79.

32. Ogilvy J.A. *Theoretical Assessmetn of the Errors Involved in Ultrasonic Location and Sizing of Molten Weld Pools* Ultrasonics, Vol 28, Iss 6, 1990, pp375-381.

33. Carlson N.M, Johnson J.A., Kunerth D.C. Control of Gmaw - *Detection of Discontinuities in the Weld Pool* Welding Journal, Vol 69, Iss 7, 1990, pp s256-s263.

34. Johnson J.A., Carlson N.M. *Weld Energy Reduction by Using Concurrent Non-Destructive Evaluation* NDT International, Vol 19, 1986, pp 190-196.

35. Calder C.A., Wilcox, W.W. *High Temperature, Noncontact Material Testing* The American Society of Mechanical Engineers, New York, NY, 1978

36. ASW Committee on Methods of Inspection *Welding Inspection* , American Welding Society, Miami FL, 1980.

37. Calder, C.A., Wilcox W.W. *Noncontact Measurement of the Elastic Constants of Plutonium at Elevated Temperatures*, Journal of Nuclear Materials, Vol 97, No 1 and 2, March 1981.